

A Li-rich $\text{Li}[\text{Li}_{0.2}\text{Ni}_{0.2}\text{Mn}_{0.6}]\text{O}_2$ Cathode Material in situ Coated with Polyaniline

Lingna Sun, Xianwen Yi, Chuan Shi, Xiangzhong Ren*, Yuan Gao, Yongliang Li, Peixin Zhang

College of Chemistry and Environmental Engineering, Shenzhen University, P.R.China, 518060)

*E-mail: renxz@szu.edu.cn

Received: 16 February 2017 / Accepted: 14 April 2017 / Published: 12 May 2017

A Li-rich $\text{Li}[\text{Li}_{0.2}\text{Ni}_{0.2}\text{Mn}_{0.6}]\text{O}_2$ cathode material coated with polyaniline (PANI) was prepared by a chemical in situ polymerization method. PANI is evenly coated on the surface of particles of the Li-rich material $\text{Li}[\text{Li}_{0.2}\text{Ni}_{0.2}\text{Mn}_{0.6}]\text{O}_2$ to form a good electrical conductive layer. The samples were characterized using X-ray diffraction (XRD), scanning electron microscopy (SEM), cyclic voltammetry (CV) and electrochemical impedance spectroscopy (EIS). When the PANI coating content was 6%, the Li-rich material exhibited a regular morphology and optimal electrochemical properties. The initial specific discharge capacity of the Li-rich material $\text{Li}[\text{Li}_{0.2}\text{Ni}_{0.2}\text{Mn}_{0.6}]\text{O}_2/\text{PANI}$ was 262.0 mAh g^{-1} at 0.1 C, and that after 50 cycles was 243.7 mAh g^{-1} , representing a capacity retention of 93% after 50 cycles.

Keywords: $\text{Li}[\text{Li}_{0.2}\text{Ni}_{0.2}\text{Mn}_{0.6}]\text{O}_2$; Polyaniline; Li-rich materials; Cathode materials.

1. INTRODUCTION

Lithium ion batteries (LIBs) are expected to be utilized for portable electronic devices and electric vehicles due to their long cycle life and high energy density [1-5]. Research on cathode materials with high performance is the focus and key problem of the development of LIBs. The applications of conventional cathode materials, such as layered LiCoO_2 and $\text{LiMn}_{1/3}\text{Ni}_{1/3}\text{Co}_{1/3}\text{O}_2$, spinel LiMn_2O_4 and olivine LiFePO_4 , are limited due to their own setbacks. Recently, lithium-rich layered Mn-based cathode materials $x\text{Li}_2\text{MnO}_3 \cdot (1-x)\text{LiMO}_2$ (M = Ni, Co, or Mn) become a potential alternative cathode material for high-capacity LIBs [6,7], as they exhibit capacities as high as 250 mAh g^{-1} [8-10].

Nonetheless, the application of Li-rich materials has been seriously restricted by their disadvantages including initial large irreversible capacities, poor rate performance, and electrolyte decomposition under high voltage. Many researchers have employed various methods, for instance, surface coating, ion doping, and particle nanocrystallization, to improve the electrochemical performance of the Li-rich cathode material and ensure battery safety under high voltage [11-15]. Surface coating is an important means that utilizes materials such as transition metal oxides, ion conductors, fluoride and conductive agents [16-18]. The coating of a carbon-based material, for example polypyrrole (PPy), polyaniline (PANI), or C itself, on the surface of a Li-rich material is also important, as it not only reduces the side reaction between the main material and electrolytic liquid via its intrinsic inertia but also enhances the electronic conductivity of the Li-rich material through the coating layer, thus improving the reversibility of the material insertion/extraction and reducing the dissolution of electrode materials in the electrolyte [19-21]. Lee's group reported the successful synthesis of $\text{Li}(\text{Mn}_{1/3}\text{Ni}_{1/3}\text{Fe}_{1/3})\text{O}_2$ -polyaniline nanocomposites by a mixed hydroxide and polymerization route and demonstrated that they exhibit outstanding rate performance [22]. Wu et al. prepared $\text{Li}_{1.2}\text{Mn}_{0.54}\text{Co}_{0.13}\text{Ni}_{0.13}\text{O}_2$ by the Pechini method and coated it with conducting PPy to improve the electrochemical performances [23]. Shi et al. studied the influence of carbon coating on the electrochemical properties of $\text{Li}_{1.048}\text{Mn}_{0.381}\text{Ni}_{0.286}\text{Co}_{0.286}\text{O}_2$ [24].

In this paper, chemical in situ polymerization was applied to coat PANI evenly on the surface of particles of the Li-rich material $\text{Li}[\text{Li}_{0.2}\text{Ni}_{0.2}\text{Mn}_{0.6}]\text{O}_2$ to form a good electrical conductive layer and thereby improve the material conductivity and electrochemical cycle performance.

2. EXPERIMENTAL

2.1. Preparation of $\text{Li}[\text{Li}_{0.2}\text{Ni}_{0.2}\text{Mn}_{0.6}]\text{O}_2/\text{PANI}$

A proper amount of $(\text{NH}_4)_2\text{S}_2\text{O}_8$ was dissolved in HCl (0.1 mol/L) and then transferred to a long neck funnel. Different contents of aniline (0%, 2%, 4%, 6%, and 8%) and the Li-rich material $\text{Li}[\text{Li}_{0.2}\text{Ni}_{0.2}\text{Mn}_{0.6}]\text{O}_2$ (prepared using a synthesis method reported earlier [25]) were added into a 0.1 mol/L HCl solution and mixed evenly, and then N_2 was pumped in for half an hour to remove the residual air the flask. Then the $(\text{NH}_4)_2\text{S}_2\text{O}_8$ solution was instilled into the aniline mixture at a controlled speed of 6 drops/min, followed by a 3 h ice bath reaction and 24 h standing. The solution was then fully washed with acetone to remove the residual hydrochloric acid and then dried for 24 h under vacuum at 60 °C to obtain the target product. All the chemicals used in the experiment, such as $(\text{NH}_4)_2\text{S}_2\text{O}_8$, HCl, $\text{MnSO}_4 \cdot 4\text{H}_2\text{O}$, $\text{NiSO}_4 \cdot \text{H}_2\text{O}$, $\text{NH}_3 \cdot \text{H}_2\text{O}$, Na_2CO_3 , $\text{LiOH} \cdot \text{H}_2\text{O}$, and aniline, were analytical grade reagents and used without further purification.

2.2. Characterization

The crystalline phase was characterized by powder X-ray diffraction (XRD, Bruker AXS D8 Advance) with Cu $\text{K}\alpha$ radiation ($\lambda = 0.15418$ nm). The morphology of the products was measured by scanning electron microscopy (SEM, Hitachi S-3400N) with energy dispersive spectroscopy (EDS).

2.3. Electrochemical measurements

The electrochemical measurements of the Li-rich materials $\text{Li}[\text{Li}_{0.2}\text{Ni}_{0.2}\text{Mn}_{0.6}]\text{O}_2/\text{PANI}$ were obtained using a coin cell (CR2032). The working electrode was synthesized by dispersing 80 wt% active material, 10 wt % acetylene black and 10 wt % polyvinylidene fluoride (PVDF) binder in N-methylpyrrolidone solvent. The liquid electrolyte was 1 mol/L LiPF_6 and carbonate (EC)/dimethyl carbonate (DMC) (1:1, by volume), a lithium metal foil was used as the negative electrode, and Celgard polymer was used as a separator. A CHI660A electrochemical workstation (CHI, USA) was used for the cyclic voltammetry tests and the AC impedance experiments. The scanning rate was 0.1 mV s^{-1} , and the scanning voltage range was 2.0-4.8 V. The galvanostatic charge-discharge tests were performed on a Land cell test system (Land CT20001A, Wuhan, China) in the voltage range of 2.0-4.6 V.

3. RESULTS AND DISCUSSION

3.1. Structure and morphological characterization

Figure 1 shows XRD patterns of the Li-rich material $\text{Li}[\text{Li}_{0.2}\text{Ni}_{0.2}\text{Mn}_{0.6}]\text{O}_2$ with different PANI-covering contents (0%, 2%, 4%, 6%, 8%), showing that a weak but orderly superlattice peak (LiMn_6) appeared when 2θ was in the range of $22\text{-}25^\circ$.

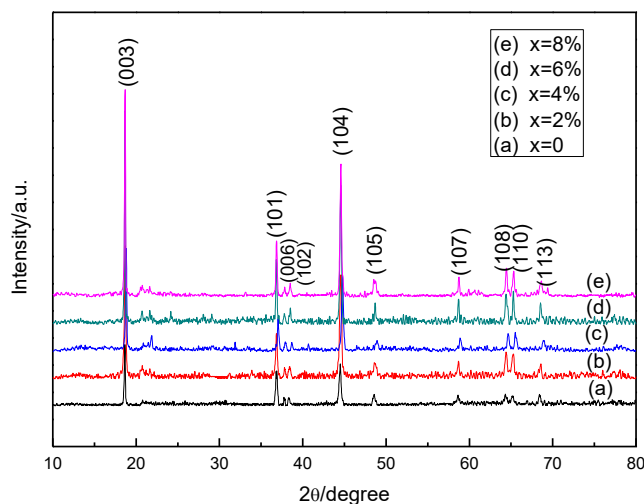


Figure 1. XRD patterns of $\text{Li}[\text{Li}_{0.2}\text{Ni}_{0.2}\text{Mn}_{0.6}]\text{O}_2/\text{PANI}$ ($x = 0\%, 2\%, 4\%, 6\%, 8\%$)

This structure was the characteristic peak of Li_2MnO_3 , and the position and intensity of the other diffraction peaks of the composite corresponded to the diffraction spectrum of an $\alpha\text{-NaFeO}_2$ layered structure, which indicates that the $\text{Li}[\text{Li}_{0.2}\text{Ni}_{0.2}\text{Mn}_{0.6}]\text{O}_2/\text{PANI}$ composite can be attributed to the hexagonal crystal and R-3m space group [26]. It can be observed that the XRD patterns of the

samples coated with polyaniline (PANI) and those not coated maintain basically the same position and intensity of the crystal diffraction peak, and no carbon-related impurity phase was found, which proves that the α -NaFeO₂ layered crystal structure did not change after PANI was coated on the Li-rich material Li[Li_{0.2}Ni_{0.2}Mn_{0.6}]O₂.

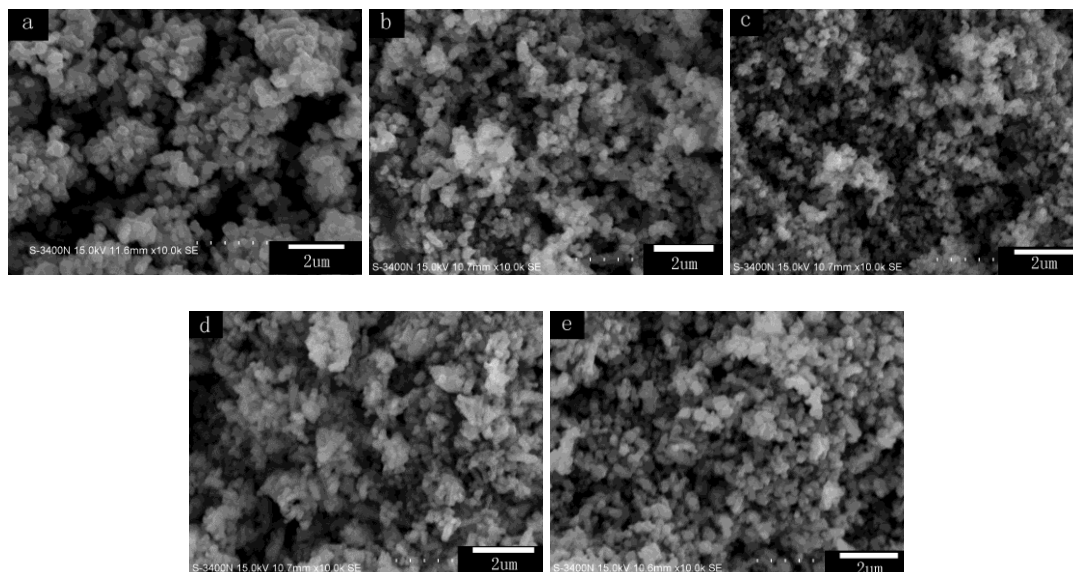
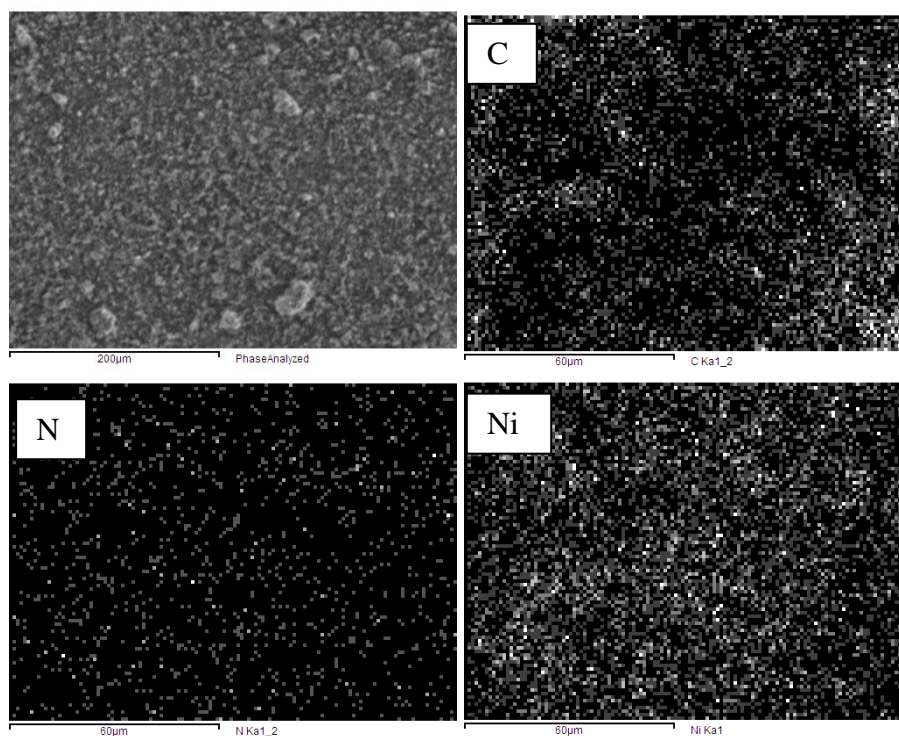


Figure 2. SEM images of Li[Li_{0.2}Ni_{0.2}Mn_{0.6}]O₂ with different contents of PANI(a = 0%; b = 2%; c = 4%; d = 6%; e = 8%)



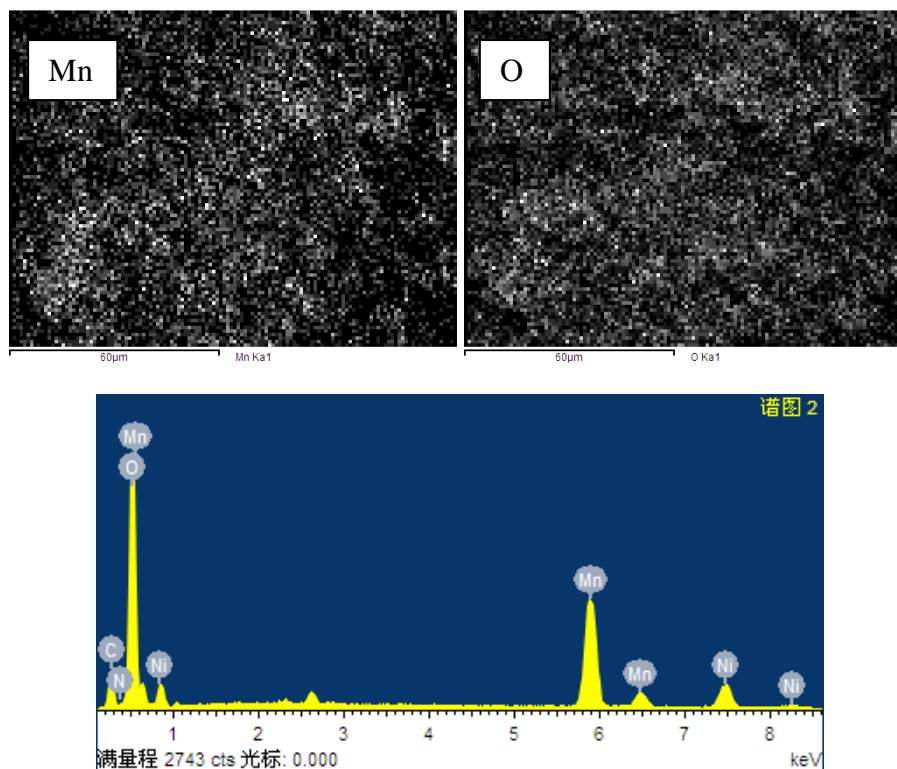


Figure 3. EDS and element mapping of $\text{Li}[\text{Li}_{0.2}\text{Ni}_{0.2}\text{Mn}_{0.6}]\text{O}_2/\text{PANI}$

Figure 2 shows SEM images of Li-rich $\text{Li}[\text{Li}_{0.2}\text{Ni}_{0.2}\text{Mn}_{0.6}]\text{O}_2/\text{PANI}$ composites with different PANI coating contents (a = 0%; b = 2%; c = 4%; d = 6%; e = 8%). The SEM images indicate that the particle surface of the pure Li-rich $\text{Li}[\text{Li}_{0.2}\text{Ni}_{0.2}\text{Mn}_{0.6}]\text{O}_2$ material was relatively smooth but became rough after being coated with PANI. When the PANI covering amount increased to 8%, the coating layer became loose and the material particles began to aggregate, which may have resulted from the aniline initially aggregating on the outer surface of the particles and the newly generated PANI growing on the coating layer when the material was added. The PANI formed a cross-linked networked structure, which led to the particle aggregation and the resulting loose surface.

Figure 3 shows the EDS and element mapping of the Li-rich $\text{Li}[\text{Li}_{0.2}\text{Ni}_{0.2}\text{Mn}_{0.6}]\text{O}_2/\text{PANI}$ composites. Peaks of C, N, Ni, Mn and O can be clearly observed in the energy spectrum graph of the $\text{Li}[\text{Li}_{0.2}\text{Ni}_{0.2}\text{Mn}_{0.6}]\text{O}_2/\text{PANI}$ composites. Through the further surface scanning of the elements, it was found that the C, N, Ni, Mn and O elements were distributed evenly on the particle surface, which confirms, to a certain extent, that the PANI was evenly coated on the surface of the $\text{Li}[\text{Li}_{0.2}\text{Ni}_{0.2}\text{Mn}_{0.6}]\text{O}_2$ particles.

3.2. Electrochemical performance

Figure 4 shows the initial charge-discharge curves of $\text{Li}[\text{Li}_{0.2}\text{Ni}_{0.2}\text{Mn}_{0.6}]\text{O}_2/\text{PANI}$ composites prepared with different PANI covering contents. A clear voltage plateau appeared when the voltage increased to 4.5 V, which corresponds to the irreversible extraction of Li_2O from the layered Li_2MnO_3

component during the charging process. When the PANI coating content was 0%, 2%, 4%, 6%, and 8%, respectively, the material's initial specific discharge capacity was 268.2, 263.9, 259.2, 262.0, and 253.7 mAh g⁻¹, and the initial charge-discharge efficiency was 74.1%, 74.9%, 73.2%, 75.8%, and 73.1%. This indicates that the initial specific discharge content of the coated material was reduced compared with that of the Li-rich material without coating. The reason may be that PANI layer separates the active material from the electrolyte. It is understandable that the discharge capacity of the coated material is slightly lower than the uncoated material because PANI is electronically conductive but insulating to the Li⁺ ions. The presence of PANI does not facilitate the Li⁺ ion transport at the surface of the solid solution [23]. When the coating content increased to 8%, the material's charge-discharge efficiency decreased, which may be a consequence of the large amount of PANI cladding that hindered the infiltration of the electrolyte into the Li-rich material.

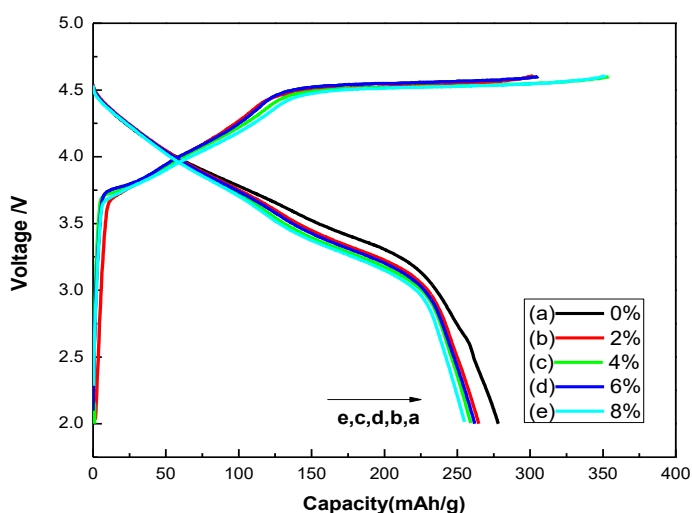


Figure 4. Initial charge-discharge curves of Li[Li_{0.2}Ni_{0.2}Mn_{0.6}]O₂/PANI($x = 0\%$, 2% , 4% , 6% , and 8%)

Figure 5 shows the cycle performance of the Li-rich material Li[Li_{0.2}Ni_{0.2}Mn_{0.6}]O₂ coated with different contents of PANI (0%, 2%, 4%, 6%, and 8%) at 0.1 C. The initial specific discharge capacities of the Li[Li_{0.2}Ni_{0.2}Mn_{0.6}]O₂ coated with proportions of PANI of 0%, 2%, 4%, 6%, and 8% were 268.2, 262.9, 259.2, 262.0, and 253.7 mAh g⁻¹, and after 50 cycles, the specific discharge capacities were, respectively, 217.0, 217.3, 228.2, 243.7, and 224.0 mAh g⁻¹, for capacity retentions of 80.9%, 82.7%, 88.0%, 93.0%, and 88.3%. Therefore the Li-rich material prepared with 6% PANI coating, possessed higher discharge capacity, and its capacity retention indicates the best cycling stability of the samples. The conducting polymer coating on the surface of Li-rich material plays an important role in improving the electrochemical performance. The reason for the electrochemical performance enhancement was that the PANI coating on the Li-rich material separated the electrode material from the electrolyte, which reduced the corrosion of the Li-rich material into the electrolyte, inhibited the dissolution of the electrode material, and reduced the transfer impedance (R_{ct}) of the Li⁺ interface charges between the solid and liquid phases during the lithium insertion/extraction to improve the stability of the layer structure in the Li-rich material Li[Li_{0.2}Ni_{0.2}Mn_{0.6}]O₂ [27]. In addition, the

electronic conductivity of $\text{Li}[\text{Li}_{0.2}\text{Ni}_{0.2}\text{Mn}_{0.6}]\text{O}_2$ increased after surface modification with PANI. It has been reported that the introduction of conductive polymer could improve the conductivity of the material and improve the cycling stability and rate properties [28-30].

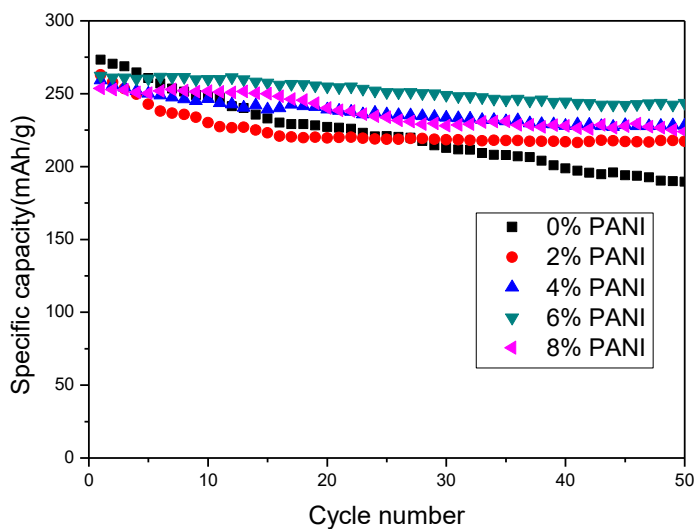


Figure 5. Cycle performance of $\text{Li}[\text{Li}_{0.2}\text{Ni}_{0.2}\text{Mn}_{0.6}]\text{O}_2$ with different contents of PANI at 0.1 C

Figure 6 is the cycle performance graphs for the pure sample and those with coating contents of 6% PANI at different rates (0.1 C, 0.2 C, 0.5 C, and 1.0 C). The initial specific discharge capacity of the Li-rich material not coated with PANI was 268.2 mAh g^{-1} , which decreased to only 221 mAh g^{-1} after 50 cycles, and the initial specific discharge capacity of that coated with PANI was 262.0 mAh g^{-1} , which was lower than that of the uncoated samples. However, the specific discharge capacity of the coated samples after 50 cycles was 239.9 mAh g^{-1} , which was higher than that of the uncoated samples. Moreover, when the PANI-coated Li-rich material was charged and discharged under high rates of 0.2 C, 0.5 C, and 1.0 C, its specific discharge capacity was higher than those of the uncoated samples. The improved rate property can be attributed to the PANI coating layer and the high conductivity of the polymer on the material surface [28,31]. During the charge-discharge process, the PANI coating layer can protect the material from harmful side reactions with the electrolyte, inhibit the dissolution of the electrode material, and thereby improve the rate performance of the Li-rich material $\text{Li}[\text{Li}_{0.2}\text{Ni}_{0.2}\text{Mn}_{0.6}]\text{O}_2$ [32]. The $\text{Li}[\text{Li}_{0.2}\text{Ni}_{0.2}\text{Mn}_{0.6}]\text{O}_2/\text{PANI}$ composites demonstrated not only better cycling stability but also higher rate performance, resulting from the PANI conductive coating layer. Thus the $\text{Li}[\text{Li}_{0.2}\text{Ni}_{0.2}\text{Mn}_{0.6}]\text{O}_2/\text{PANI}$ composites exhibit superior electrochemical properties in comparison to $\text{Li}(\text{Mn}_{1/3}\text{Ni}_{1/3}\text{Fe}_{1/3})\text{O}_2/\text{PANI}$ [22], $\text{Li}_{1.2}\text{Mn}_{0.54}\text{Co}_{0.13}\text{Ni}_{0.13}\text{O}_2/\text{PPy}$ [23], $\text{Li}[\text{Li}_{0.1}\text{Ni}_{0.45}\text{Mn}_{0.45}]\text{O}_2/\text{graphene}$ [6] (Table 1).

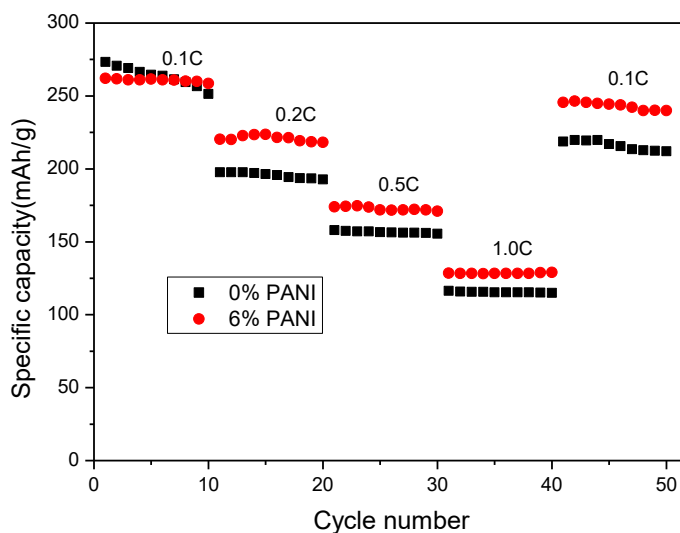


Figure 6. Discharge rate capabilities of $\text{Li}[\text{Li}_{0.2}\text{Ni}_{0.2}\text{Mn}_{0.6}]\text{O}_2$ with different PANI coating contents: (a) 0% PANI and (b) 6% PANI.

Table 1. Electrochemical performance of various Li-rich layered oxides material /carbon materials for LIBs.

Materials	Current density	Cycle number	Specific capacity (mAh g^{-1})	Reference
$\text{Li}_{1.2}\text{Ni}_{0.2}\text{Mn}_{0.6}\text{O}_2/\text{PEDOT:PSS}$	1C	100	146.9	[28]
$\text{Li}(\text{Mn}_{1/3}\text{Ni}_{1/3}\text{Fe}_{1/3})\text{O}_2/\text{PANI}$	0.5C	40	155	[22]
$\text{Li}_{1.2}\text{Mn}_{0.54}\text{Co}_{0.13}\text{Ni}_{0.13}\text{O}_2/\text{PPy}$	12.5mA/g	30	220	[23]
$\text{Li}[\text{Li}_{0.1}\text{Ni}_{0.45}\text{Mn}_{0.45}]\text{O}_2/\text{graphene}$	0.1C	50	210	[6]
$\text{Li}[\text{Li}_{0.2}\text{Ni}_{0.2}\text{Mn}_{0.6}]\text{O}_2/\text{PANI}$	0.1C	50	239.9	This work

Figure 7 is the third CV curve of the Li-rich material $\text{Li}[\text{Li}_{0.2}\text{Ni}_{0.2}\text{Mn}_{0.6}]\text{O}_2$ coated with different PANI proportions (0%, 2%, 4%, 6%, 8%). Through the comparison of the cyclic voltammetry curves before and after the PANI coating, it can be found that three anodic peaks and two cathodic peaks were included in the CV curve, which indicates that the structure and $\text{Ni}^{2+}/\text{Ni}^{4+}$ phase transformation of the Li-rich material $\text{Li}[\text{Li}_{0.2}\text{Ni}_{0.2}\text{Mn}_{0.6}]\text{O}_2$ before and after the PANI coating were kept stable during the insertion/extraction, and the electrochemical reaction system of lithium insertion/extraction did not change after the PANI coating. A reduction peak of $\text{Mn}^{4+} \rightarrow \text{Mn}^{3+}$ appeared at approximately 3.35 V, while a corresponding weak anodic peak appeared at 3.5 V. The potential difference when coated with PANI is $\Delta\phi = 0.15$ V, smaller than the 0.2 V for that not coated, and the peak current becomes small,

indicating that the activation of the Mn^{4+} in the material is inhibited after the PANI coating, which reduces the dissolution of the Li-rich manganese base Li_2MnO_3 in the electrolyte to maintain the stability of the layer structure in the subsequent electrochemical lithium insertion/extraction process [33,34].

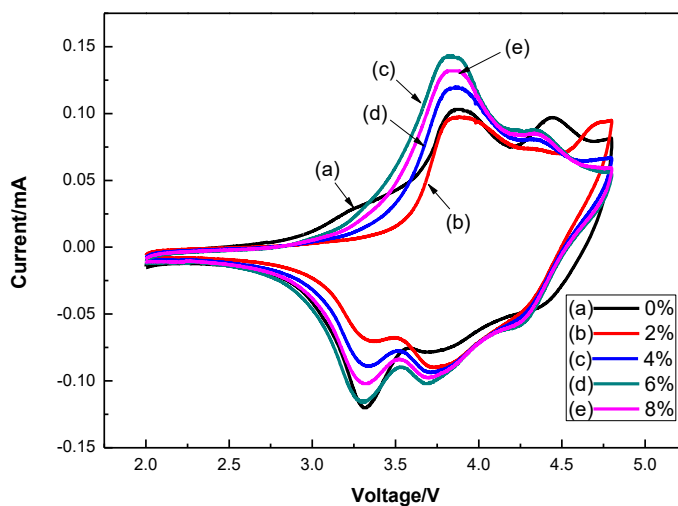


Figure 7. Cyclic voltammety curves of $Li[Li_{0.2}Ni_{0.2}Mn_{0.6}]O_2$ coated with different contents of PANI ($x = 0\%, 2\%, 4\%, 6\%, 8\%$)

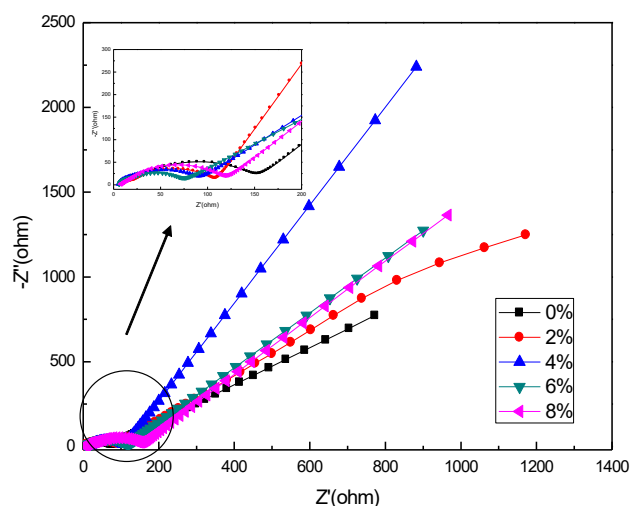


Figure 8. Nyquist plots of $Li[Li_{0.2}Ni_{0.2}Mn_{0.6}]O_2$ with different PANI coating contents

To further explore the influence of the PANI coating on the Li^+ diffusion rate in the Li-rich material, electrochemical impedance spectroscopy (EIS) needs to be used for research on the electrochemical mechanism. The experiment investigated the influence of the different PANI coating contents (0%, 2%, 4%, 6%, and 8%) on the Li-rich material $Li[Li_{0.2}Ni_{0.2}Mn_{0.6}]O_2$ EIS. Figure 8 shows

the EIS of the different PANI coating contents (0%, 2%, 4%, 6%, and 8%), and the fitting results were as shown in Table 2.

Table 2. Fitting results of the impedance parameters of $\text{Li}[\text{Li}_{0.2}\text{Ni}_{0.2}\text{Mn}_{0.6}]\text{O}_2$ with different PANI coating contents

Coating content	Re(Ω)	CPE(sf+dl)(Ω)	Rct(Ω)
0	6.342	22.28	114.6
2%	5.768	18.17	89.97
4%	5.214	16.52	61.48
6%	5.782	13.89	52.35
8%	6.579	16.58	89.97

According to Table 2, after the $\text{Li}[\text{Li}_{0.2}\text{Ni}_{0.2}\text{Mn}_{0.6}]\text{O}_2$ material was coated with different contents of PANI, the charge transfer impedances Rct were 114.60, 89.97, 61.48, 49.15, and 89.97 Ω . After coating with PANI, the electrochemical transfer impedances of the Li-rich material were all smaller than 114.6 Ω for the uncoated material. The material's charge transfer impedance reached the minimum when the PANI coating content was 6% and increased at 8%, indicating that the charge transfer impedance of the Li^+ at the interface was clearly reduced after being coated with a proper amount of PANI, consistent with the improvement of the material's electrochemical cycle performance. The reason could be that PANI is a conductive polymer that can improve the material's electronic conductivity. Additionally, as an inert material, it can inhibit the direct contact between the electrode material and electrolyte, thus reducing the occurrence of side reactions between the Li-rich material and electrolyte and improving the Li^+ diffusion rate and the material's electrochemical properties.

4. CONCLUSION

Chemical in situ polymerization was used to prepare a Li-rich $\text{Li}[\text{Li}_{0.2}\text{Ni}_{0.2}\text{Mn}_{0.6}]\text{O}_2/\text{PANI}$ composite. Upon coating with PANI, the Li-rich layer structure did not change, and the Li-rich particles still maintained their grain morphology. However, an excessive coating content could cause material agglomeration. The experiment explored the influence of the PANI coating content on the crystal structure and electrochemical properties of the Li-rich material. When the coating content was 6%, the Li-rich material maintained a regular morphology and optimal electrochemical properties. When the Li-rich material $\text{Li}[\text{Li}_{0.2}\text{Ni}_{0.2}\text{Mn}_{0.6}]\text{O}_2/\text{PANI}$ was at 0.1 C, the initial specific discharge capacity and that after 50 cycles were 262.0 and 243.7 mAh g^{-1} , respectively, representing a capacity retention of 93% after 50 cycles, which was higher than that of the uncoated cathode materials.

ACKNOWLEDGEMENTS

This work was financially supported by the National Natural Science Foundation of China (21671136, 21471100, 51502177, 21601126), the Natural Science Foundation of Guangdong (2015A030313542, 2016A030313057), Training Foundation for Outstanding Young Teachers in Higher Education Institutions of Guangdong (YQ2015146).

References

1. S. Kim, D. Seo, X. Ma, G. Ceder and K. Kang, *Adv. Energy Mater.*, 2 (2012) 710.
2. N. Choi, Z. Chen, S. Freunberger, X. Ji, Y. Sun, K. Amine, G. Yushin, L. Nazar, J. Cho and P. Bruce, *Angew. Chem. Int. Ed.*, 51 (2012) 9994.
3. C. Hayner, X. Zhao and H. Kung, *Annu. Rev. Chem. Biomol. Eng.*, 3 (2012) 445.
4. J. Goodenough and Y. Kim, *Chem. Mater.*, 22 (2010) 587.
5. V. Etacheri, R. Marom, R. Elazari, G. Salitra and D. Aurbach, *Energy Environ. Sci.*, 4 (2011) 3243.
6. H. Zhuo, Y. Zhang, D. Wang, C. He, C. Zhu, Q. Zhang, C. Li, L. Sun, J. Liu and S. Chen, *Electrochim. Acta.*, 149 (2014) 42.
7. C. Wang, F. Zhou, K. Chen, J. Kong, Y. Jiang, G. Yan, J. Li, C. Yu and W. Tang, *Electrochim. Acta.*, 176 (2015) 1171.
8. C. Johnson, J. Kim, C. Lefief, N. Li, J. Vaughey and M. Thackeray, *Electrochem. Commun.*, 6 (2004) 1085.
9. A. Ito, D. Li, Y. Ohsawa and Y. Sato, *J. Power Sources*, 183 (2008) 344.
10. M. Thackeray, S. Kang, C. Johnson, J. Vaughey, R. Benedeka and S. Hackney, *J. Mater. Chem.*, 17 (2007) 3112.
11. Y. Liu, J. Lv, S. Liu, L. Chen and X. Chen, *Powder Technol.*, 239 (2013) 461.
12. S. Kang, H. Qin, Y. Fang, X. Li and Y. Wang, *Electrochim. Acta.*, 144 (2014) 22.
13. T. Tang and H. Zhang, *Electrochim. Acta.*, 191 (2016) 263.
14. Y. Zhao, M. Xia, X. Hu, Z. Zhao, Y. Wang and Z. Lv, *Electrochim. Acta.*, 174 (2015) 1167.
15. Y. Zang, C. Ding, X. Wang, Z. Wen and C. Chen, *Electrochim. Acta.*, 168 (2015) 234.
16. D. Lee, B. Scrosati and Y. Sun, *J. Power Sources*, 196 (2011) 7742.
17. Y. Zhao, C. Zhao, H. Feng, Z. Sun and D. Xia, *Electrochem. Solid-State Lett.*, 14 (2011) A1.
18. S. Kang and M. Thackeray, *Electrochem. Commun.*, 11 (2009) 748.
19. D. Tong, Q. Lai, N. Wei, A. Tang, L. Tang, K. Huang and X. Ji, *Mater. Chem. Phys.*, 94 (2005) 432.
20. A. Manthiram, *J. Phys. Chem. Lett.*, 2 (2011) 176.
21. D. Kim, E. Lee, M. Slater, W. Lu, S. Rood and C. Johnson, *Electrochem. Commun.*, 18 (2012) 66.
22. K. Karthikeyan, S. Amaresh, V. Aravindan, W. Kim, K. Nam, X. Yang and Y. Lee, *J. Power Sources*, 232 (2013) 240.
23. C. Wu, X. Fang, X. Guo, Y. Mao, J. Ma, C. Zhao, Z. Wang and L. Chen, *J. Power Sources*, 231 (2013) 44.
24. S. Shi, J. Tu, Y. Mai, Y. Zhang, C. Gu and X. Wang, *Electrochim. Acta.*, 63 (2010) 112.
25. L. Sun, X. Yi, X. Ren, P. Zhang and J. Liu, *J. Electrochem. Soc.*, 163 (2016) A766.
26. H. Kitaura, A. Hayashi, K. Tadanaga and M. Tatsumisago, *Electrochim. Acta.*, 55 (2010) 8821.
27. X. Yin, C. Li, M. Zhang, Q. Hao, S. Liu, L. Chen and T. Wang, *J. Phys. Chem. C*, 114 (2010) 8084.
28. F. Wu, J. Liu, L. Li, X. Zhang, R. Luo, Y. Ye and R. Chen, *ACS Appl. Mater. Interfaces* 8 (2016) 23095.
29. T. Higgins, S. Park, P. King, C. Zhang, N. McEvoy, N. Berner, D. Daly, A. Shmeliov, U. Khan, G. Duesberg, V. Nicolosi, and J. Coleman, *ACS Nano*, 10 (2016) 3702.

30. G. Xu, Y. Li, T. Ma, Y. Ren, H. Wang, L. Wang, J. Wen, D. Miller, K. Amine and Z. Chen, *Nano Energy*, 18 (2015) 253.
31. D. Yoon, S. Yoon, K. Ryu and Y. Park, *Sci. Rep.*, 6 (2016) 19962.
32. X. Bian, Q. Fu, Q. Pang, Y. Gao, Y. Wei, B. Zou, F. Du and G. Chen, *ACS Appl. Mater. Interfaces*, 8 (2016) 3308.
33. K. Tan, M. Reddy, G. Rao and B. Chowdari, *J. Power Sources*, 41 (2005) 129.
34. T. Zhao, L. Li, S. Chen, R. Chen, X. Zhang, J. Lu, F. Wu and K. Amine, *J. Power Sources*, 245 (2014) 898.

© 2017 The Authors. Published by ESG (www.electrochemsci.org). This article is an open access article distributed under the terms and conditions of the Creative Commons Attribution license (<http://creativecommons.org/licenses/by/4.0/>).